Metagenome of a Versatile Chemolithoautotroph from Expanding Oceanic Dead Zones

David A. Walsh, *et al.*

Science **326**, 578 (2009);
DOI: 10.1126/science.1175309

CORRECTED 30 APRIL 2010; SEE LAST PAGE

granule neurons (Fig. 2J and fig. S6F). Thus, NeuroD2 knockdown increases the density of functionally active sites of presynaptic differentiation.

In gain-of-function analyses, expression of the mutant NeuroD2 protein ND2-DBM in neurons reduced the density of presynaptic sites (Fig. 2K and fig. S7, A to C). In epistasis analyses, NeuroD2 knockdown suppressed the effect of Cdc20 knockdown on presynaptic differentiation (Fig. 2L and fig. S7, D and E). These results suggest that Cdc20-APC promotes the formation of functional presynaptic axonal sites through NeuroD2 degradation in neurons.

Among the reported NeuroD2 targets is the gene encoding Complexin II (Cplx2), a protein that modulates synaptic vesicle fusion to the presynaptic membrane in invertebrates (*9*, *10*). We asked if Cplx2 might mediate NeuroD2-dependent control of presynaptic differentiation. Knockdown of Cplx2 robustly increased the density of synapsin clusters in granule neurons, and this phenotype was reversed by expression of Cplx2 encoded by an RNAi-resistant cDNA (Cplx2-RES) but not wild-type cDNA (Cplx2-WT) (Fig. 3A and fig. S8, A and B). Cplx2 knockdown also increased the density of functionally active presynaptic axonal sites in granule neurons (Fig. 3, B to D, and fig. S8, C to F). Finally, Cplx2 knockdown increased synapsin cluster density in granule neuron parallel fiber axons in the cerebellar cortex in slices (fig. S8G). Thus, Cplx2 knockdown phenocopies the effect of NeuroD2 knockdown on presynaptic differentiation.

In epistasis analyses, expression of exogenous Cplx2 in granule neurons reduced the density of functionally active presynaptic sites induced by NeuroD2 RNAi (Fig. 3E and fig. S9, A and B). Further, although knockdown of NeuroD2 or Cplx2 each stimulated presynaptic differentiation, the combination of NeuroD2 and Cplx2 knockdown together did not additively increase the density of presynaptic sites (Fig. 3F and fig. S9, C and D). In other experiments, knockdown of Cplx2 reversed Cdc20 RNAi-induced suppression of presynaptic differentiation (Fig. 3G and fig. S9, E and F). Collectively, these results suggest that Cplx2 mediates the ability of NeuroD2 to suppress presynaptic differentiation and acts as a downstream component of the Cdc20-APC pathway in the control of presynaptic development.

We next determined the role of the Cdc20-APC ubiquitin signaling pathway in presynaptic differentiation in the developing organism. To visualize the morphogenesis of presynaptic axonal differentiation in vivo, we expressed GFP in the cerebellar cortex in rat pups using an electroporation method (*3*, *5*, *11*). These analyses revealed granule neuron cell bodies in the internal granule layer (IGL) and their parallel fiber axons in the molecular layer (ML) (Fig. 4A). Parallel fiber axons displayed varicosities along the axon (Fig. 4B), which colocalized with punctate synapsin immunoreactivity and were apposed to punctate PSD-95, a marker of postsynaptic structures (Fig. 4B). These observations indicate that parallel fiber axon varicosities represent sites of presynaptic axonal differentiation in vivo.

Using electroporation, we next induced knockdown of Cdc20, NeuroD2, or Cplx2 in rat pups. Cdc20 knockdown reduced the density of presynaptic parallel fiber varicosities in the cerebellar cortex in vivo. In contrast, knockdown of NeuroD2 or Cplx2 in rat pups increased the density of presynaptic varicosities in the cerebellar cortex (Fig. 4C and fig. S10). These results suggest that the Cdc20-APC ubiquitin signaling pathway cell-autonomously regulates presynaptic axonal differentiation in the developing brain in vivo.

We have identified a Cdc20-APC ubiquitin ligase signaling pathway that orchestrates presynaptic development and hence the establishment of neuronal circuitry in the brain (see model in fig. S11). APC function in cell cycle control has been the subject of intense scrutiny (*8*). Whereas Cdh1-APC operates in late mitosis and G1 phase of the cell cycle, Cdc20-APC controls the transition of the cell cycle through early mitosis (*8*). In the control of axon morphogenesis in postmitotic neurons, Cdh1-APC appears to control axon growth and patterning (*3*), whereas Cdc20-APC operates at a later developmental stage to promote presynaptic axonal differentiation. Thus, in an analogous manner to the temporal control of the cell cycle, the APC in concert with its two different coactivators, Cdh1 and Cdc20, appears to govern distinct temporal phases of axon differentiation in postmitotic neurons in the brain.

References and Notes

1. A. DiAntonio, L. Hicke, *Annu. Rev. Neurosci.* **27**, 223 (2004).
2. Y. Jin, C. C. Garner, *Annu. Rev. Cell Dev. Biol.* **24**, 237 (2008).
3. Y. Konishi, J. Stegmuller, T. Matsuda, S. Bonni, A. Bonni, *Science* **303**, 1026 (2004).
4. A. H. Kim *et al.*, *Cell* **136**, 322 (2009).
5. Materials and methods are available as supporting material on *Science* Online.
6. P. Chi, P. Greengard, T. A. Ryan, *Nat. Neurosci.* **4**, 1187 (2001).
7. K. I. Willig, S. O. Rizzoli, V. Westphal, R. Jahn, S. W. Hell, *Nature* **440**, 935 (2006).
8. J. M. Peters, *Nat. Rev. Mol. Cell Biol.* **7**, 644 (2006).
9. C. H. Lin *et al.*, *Proc. Natl. Acad. Sci. U.S.A.* **102**, 14877 (2005).
10. S. Huntwork, J. T. Littleton, *Nat. Neurosci.* **10**, 1235 (2007).
11. A. Shalizi *et al.*, *Science* **311**, 1012 (2006).
12. M. A. Xu-Friedman, K. M. Harris, W. G. Regehr, *J. Neurosci.* **21**, 6666 (2001).

13. We thank members of the Bonni laboratory for helpful discussions. This work was supported by NIH grants NS051255 and NS041021 (A.B.); a NSF fellowship, the Lefler Fellowship, and the Ryan Foundation (Y.Y.); a National Research Service Award Research Training grant, National Cancer Institute, and Brain Science Foundation grant (A.H.K.); the Japan Society for the Promotion of Science (T.Y.); and a Human Frontier Science Program long-term fellowship (Y.I.).

Supporting Online Material

www.sciencemag.org/cgi/content/full/326/5952/575/DC1
Materials and Methods
Figs. S1 to S13
References

1 June 2009; accepted 3 September 2009
10.1126/science.1177087

Metagenome of a Versatile Chemolithoautotroph from Expanding Oceanic Dead Zones

David A. Walsh,[1] Elena Zaikova,[1] Charles G. Howes,[1] Young C. Song,[1] Jody J. Wright,[1] Susannah G. Tringe,[2] Philippe D. Tortell,[3,4] Steven J. Hallam[1,5]*

Oxygen minimum zones, also known as oceanic "dead zones," are widespread oceanographic features currently expanding because of global warming. Although inhospitable to metazoan life, they support a cryptic microbiota whose metabolic activities affect nutrient and trace gas cycling within the global ocean. Here, we report metagenomic analyses of a ubiquitous and abundant but uncultivated oxygen minimum zone microbe (SUP05) related to chemoautotrophic gill symbionts of deep-sea clams and mussels. The SUP05 metagenome harbors a versatile repertoire of genes mediating autotrophic carbon assimilation, sulfur oxidation, and nitrate respiration responsive to a wide range of water-column redox states. Our analysis provides a genomic foundation for understanding the ecological and biogeochemical role of pelagic SUP05 in oxygen-deficient oceanic waters and its potential sensitivity to environmental changes.

Dissolved oxygen (O_2) concentration is a critical determinant of marine ecosystem structure and function. O_2 deficiency results in habitat compression and reduced productivity for aerobic organisms, with concomitant expansion of conditions favoring chemolithotrophic energy metabolism (*1*), which results in nitrogen loss and production of climate-active trace gases such as nitrous oxide (N_2O) and methane (CH_4) (*2*, *3*). Extensive oxygen minimum zones (OMZs), defined by O_2 concentrations < 20 μM, are found throughout the eastern North Pacific (ENP), eastern South Pacific (ESP), northern Indian Ocean, and southwest African shelf waters (*3*). Moreover, climate change–induced expansion and intensification of OMZs is occurring globally, with potentially deleterious effects on oceanic nitrogen cycling and carbon sequestration (*1*, *4*–*6*).

Although the extent of oxygen deficiency varies among OMZs, taxonomic surveys reveal conserved patterns of microbial community composition (*7*–*9*). In all sites examined, small subunit ribosomal RNA (SSU rRNA) gene libraries are enriched with sequences affiliated with chemoautotrophic gill symbionts of deep-sea clams and mussels (ESP-OMZ-sequence-accumulation–1 (EOSA-1) in the ESP and gamma-proteobacterial sulfur oxidizer (GSO) cluster in African shelf waters) (*9*–*11*). Phylogenetic analyses indicate that the GSO–EOSA-1 complex consists of two closely related, cooccurring and uncultivated lineages, ARCTIC96BD-19 (*12*) and SUP05 (*13*), with the latter encompassing the symbionts (Fig. 1, A and B). Blooming SUP05 populations have recently been implicated in chemolithotrophic sulfide (H_2S) oxidation coupled to nitrate (NO_3^-) reduction in African shelf waters (*10*). Both ARCTIC96BD-19 and SUP05 populations are also found in nonsulfidic waters of the ENP and ESP, which suggests that they can adopt alternative modes of energy metabolism. Given the potential importance of ARCTIC96BD-19 and SUP05 to carbon, nitrogen, and sulfur cycling in OMZs, a deeper understanding of the metabolic capabilities of these lineages is needed to constrain their respective ecological and biogeochemical roles.

Saanich Inlet, British Columbia, is a seasonally anoxic fjord characterized by an annual stratification and deep-water renewal cycle (*14*), resulting in large water-column redox gradients and high rates of trace gas production and consumption (fig. S1, A to C). Previously, we identified pelagic SUP05 in the Saanich Inlet water column, representing up to 37% of total bacteria (table S1) (*11*). Further examination of SUP05 SSU rRNA gene copy number during seasonal stratification revealed blooming populations below the oxycline, reaching up to 4.75×10^5 copies per ml in regions of H_2S and NO_3^- depletion (*15*) (fig. S2). High-resolution SSU rRNA gene surveys revealed two SUP05 phylotypes, SI-1 and SI-2 (Figs. 1A and 2A), differing by ~4% nucleotide identity. Although SI-1 dominated suboxic waters year round, SI-2 was less common, and transiently increased during deep-water renewal events, which indicated ecologically differentiated populations (Fig. 2A). Here we analyzed 16 bi-directionally end-sequenced fosmid libraries constructed from environmental DNA samples spanning oxic to anoxic waters over the seasonal stratification and deep-water renewal cycle in order to reconstruct the metabolic potential of uncultivated pelagic SUP05 populations (fig. S1D).

To identify SUP05-specific scaffolds, fosmid paired-end sequences were assembled and binned on the basis of shared sequence similarity to symbiont reference genomes (*16*, *17*) and analysis of intrinsic oligonucleotide composition patterns (fig. S3). Nineteen scaffolds encompassing 1.16 million base pairs of SUP05 DNA (SUP05 metagenome) were identified (table S2) and taxonomically verified (table S3). Consistent with SSU rRNA gene survey data, a majority of fosmid paired-end sequences within SUP05 scaffolds were derived from samples exhibiting elevated SI-1 phylotype abundance (Fig. 2B). Of

[1]Department of Microbiology and Immunology, University of British Columbia, Vancouver, BC V6T 1Z4, Canada. [2]Department of Energy Joint Genome Institute, Walnut Creek, CA 94598, USA. [3]Department of Earth and Ocean Sciences, University of British Columbia, Vancouver, BC V6T 1Z4, Canada. [4]Department of Botany, University of British Columbia, Vancouver, BC V6T 1Z4, Canada. [5]University of British Columbia Graduate Program in Bioinformatics, Vancouver, BC V6T 1Z4, Canada.

*To whom correspondence should be addressed. E-mail: shallam@interchange.ubc.ca

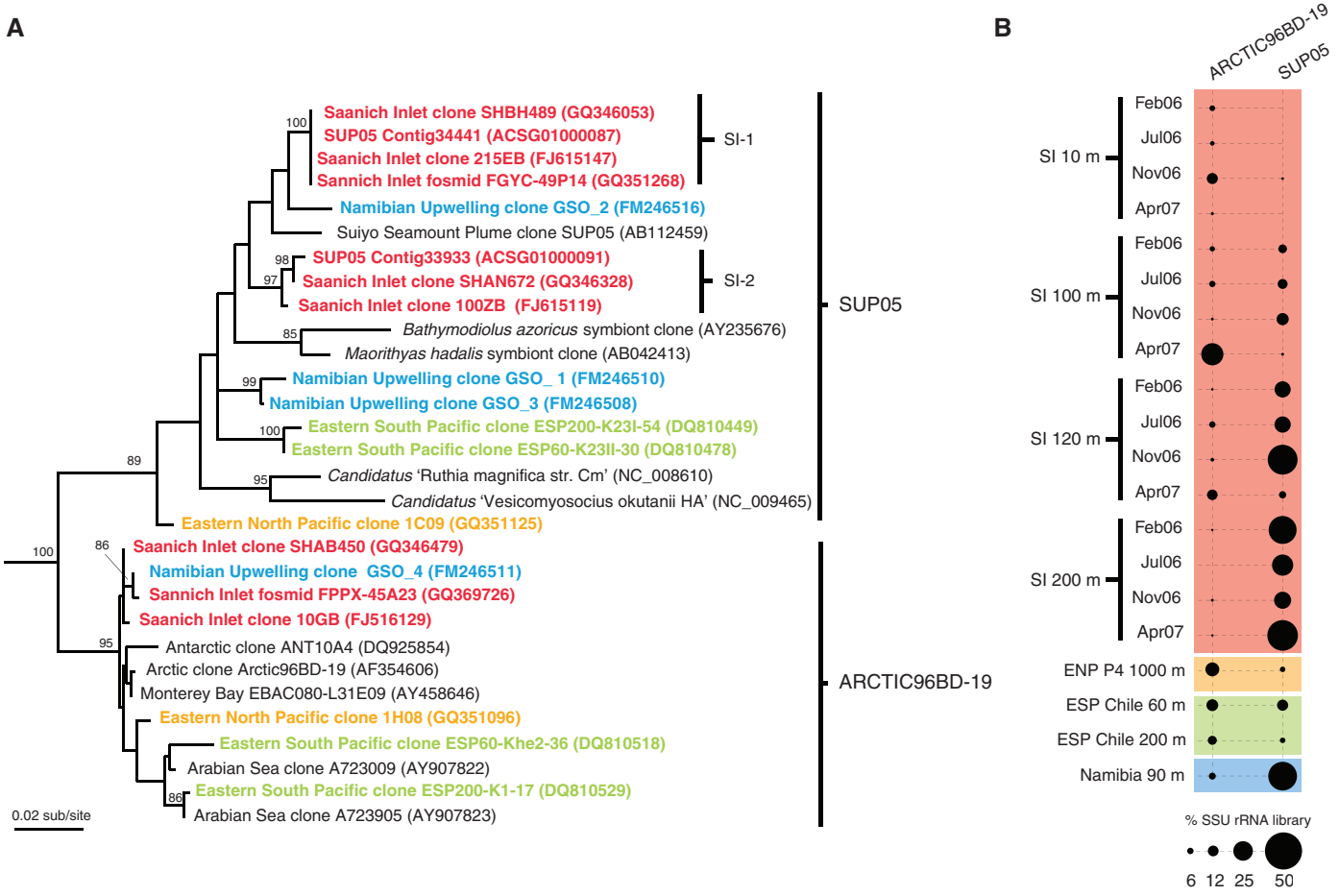

Fig. 1. (**A**) Phylogenetic tree of ARCTIC96BD-19 and SUP05 lineages based on comparative SSU rRNA gene analysis. The tree was inferred using maximum likelihood implemented in PHYML. (**B**) Relative abundance of ARCTIC96BD-19 and SUP05 SSU rRNA sequences recovered from Saanich Inlet (SI), eastern North Pacific (ENP), eastern South Pacific (ESP) (*9*), and southwest African shelf waters (Namibia) (*10*).

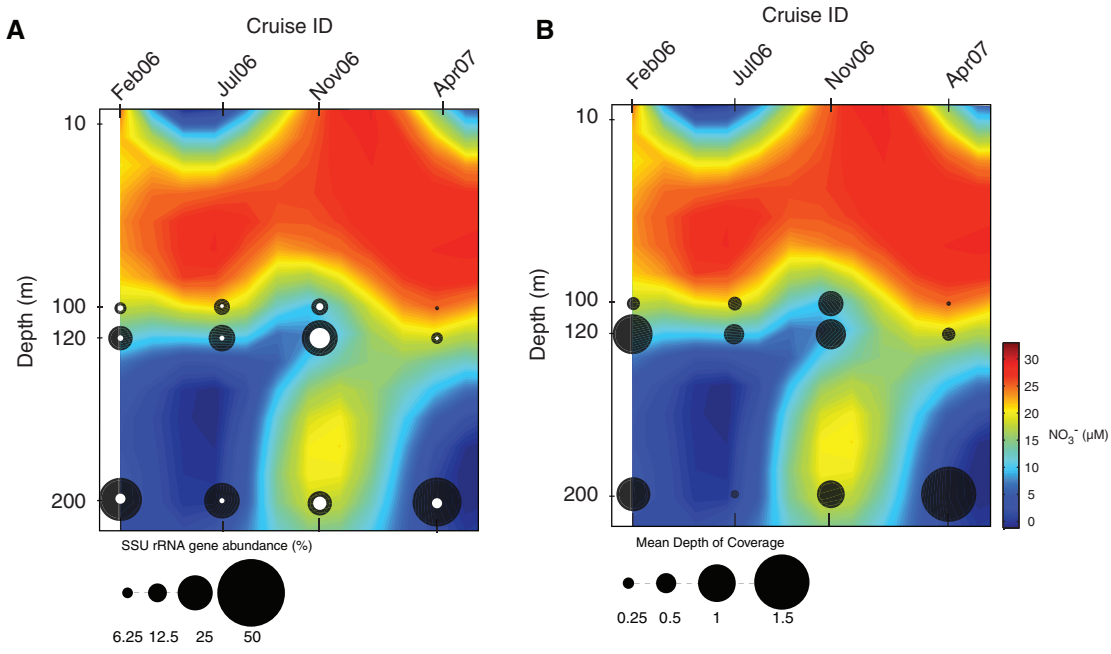

Fig. 2. (**A**) Phylotype abundance of SUP05 SI-1 (black circles) and SI-2 (white circles) based on recovery of SSU rRNA gene sequences in PCR-generated clone libraries. (**B**) Mean depth of coverage of the SUP05 metagenome plotted over the Saanich Inlet nitrate profile during the 2006–07 season. Sample dates and depths are noted on the *x* and *y* axes, respectively.

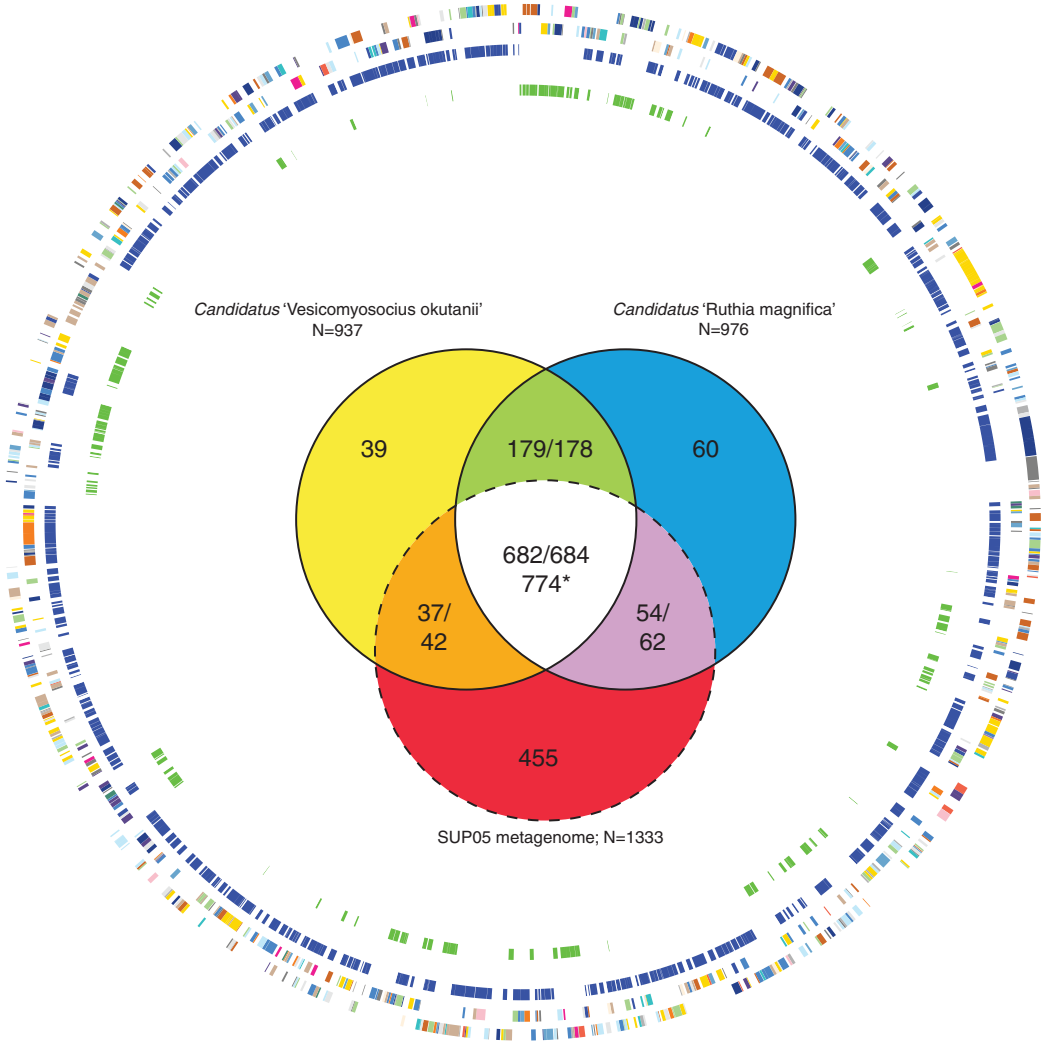

Fig. 3. Gene content comparison between SUP05 metagenome and symbiont reference genomes. Nested circles from outermost to innermost represent the following: (i and ii) Functional predictions based on clusters of orthologous groups (COG) on the forward and reverse strands of the *R. magnifica* reference genome (see fig. S4 for COG color code designation). (iii) Conservation of gene content and (iv) genes conserved in symbionts, but absent from the SUP05 metagenome. (**Inset**) Venn diagram depicts predicted gene distribution among SUP05 metagenome and symbiont reference genomes. Values correspond to the number of shared genes among overlapping genomes, with each genome used as the original query. The dotted line represents the open-genome configuration of the SUP05 metagenome. *The discrepancy in core size when SUP05 metagenome is used as query (774) compared with symbionts (~683) reflects gene content redundancy in the metagenome assembly.

861 genes shared between symbiont reference genomes, 80% were conserved in the SUP05 metagenome (supporting online material text, Fig. 3 and fig. S4). Many of these genes are predicted to mediate informational processing steps, particularly translation, although a significant fraction function in carbon, sulfur, amino acid, and coenzyme metabolism (figs. S5 and S6). Approximately 35% of gene content predicted in the SUP05 metagenome was unique, including genes implicated in DNA uptake and repair, denitrification, and adaptive or stress responses (*15*).

Similar to symbiotic counterparts, the SUP05 metagenome harbors genes mediating the Calvin-Benson-Bassham (CBB) cycle for autotrophic carbon assimilation, including a single form II ribulose-1,5-bisphosphate carboxylase-oxygenase (RuBisCO) gene, which both implicate SUP05 in chemosynthetic carbon fixation (*18*). In addition, a gene encoding β-class carbonic anhydrase, a potential CO_2-concentrating mechanism, was also identified. The repertoire of genes required for converting fixed carbon to hexose and ribose sugars via gluconeogenesis and the nonoxidative branch of the pentose phosphate pathway were identified, along with the majority of tricarboxylic acid (TCA) cycle components (fig. S6). However, we did not recover genes for enzymes mediating the interconversion of succinyl-CoA and 2-oxoglutarate (fig. S6), which indicated that SUP05 is potentially an obligate autotroph as posited earlier for clam symbionts (*16*, *17*).

From the standpoint of energy metabolism, the SUP05 metagenome harbors a diverse repertoire of genes involved in chemolithotrophic oxidation of reduced sulfur compounds. We found genes encoding flavocytochrome c sulfide dehydrogenase (*fccAB*) and sulfide quinone oxidoreductase (*sqr*), mediating oxidation of H_2S to elemental sulfur (S^0) (fig. S6). The presence of two enzymatic complexes may facilitate sulfur-based energy metabolism under variable sulfide regimes. In addition, dissimilatory sulfite reductase subunits (*dsrAB*), adenosine 5′-phosphosulfate (APS) reductase (*apr*), and adenosine 5′-triphosphate (ATP) sulfurylase (*sat*) mediating complete oxidation of S^0 to sulfate, and the Sox pathway (*soxABXYZ*) for thiosulfate ($S_2O_3^{2-}$) oxidation (fig. S6) (*19*) were conserved between pelagic SUP05 and symbiont reference genomes. The capacity to obtain electrons from $S_2O_3^{2-}$ may be of ecological relevance, given that mixing of sulfidic and oxygenated water masses results in $S_2O_3^{2-}$ accumulation owing to chemical oxidation of H_2S (*20*, *21*). Moreover, the apparent absence of *soxCD* sulfur dehydrogenase genes indicates the capacity to store S^0, which can be subsequently oxidized via the reverse dissimilatory sulfate reduction (DSR) pathway and thereby provisions SUP05 in the absence of ambient reductant (*22*). Indeed, *soxCD* homologs are also absent from symbiont reference genomes, and colloidal sulfur globule formation has been associated with a subset of clam symbionts (*23*).

Although symbiont reference genomes harbor multiple aerobic respiratory complexes (*16*, *17*), none were recovered in the SUP05 metagenome, consistent with a facultative or strictly anaerobic life-style. Indeed, all enzymatic machinery needed to reduce NO_3^- to nitrous oxide (N_2O), including membrane-bound (*narKK2GHJI*) and periplasmic (*napFBAHGD*) dissimilatory nitrate reductases, which potentially operate under high and low NO_3^- conditions, respectively (*24*, *25*); copper-containing nitrite reductase (*nirK*); and N_2O forming nitric oxide reductase (*norCB*) (Fig. 4 and fig. S6), were identified, which mechanistically implicated pelagic SUP05 in biological nitrogen loss from oxygen-deficient oceanic waters. Moreover, the genomic colocalization of sulfur oxidation and denitrification genes in close proximity to Crp/Fnr transcriptional regulators (Fig. 4) may allow coordinated gene expression in response to changing redox states or nutrient limitation (*24*, *26*, *27*).

We identified more than 10 putative toxin-antitoxin (TA) modules in the SUP05 metagenome, which indicated a highly regulated stress response (table S4). TA modules consist of a stable toxin and a labile antitoxin and are commonly associated with environmental bacteria, where they control induction of reversible cellular stasis (*28*). Of specific interest is a TA module of the RelE superfamily identified within an operon encoding molybdopterin-guanine dinucleotide synthase (*mobA*) (Fig. 4). The product of MobA, molybdopterin-guanine dinucleotide (MGD), is an essential cofactor for all described classes of nitrate reductase (*29*), and therefore, *mobA* expression is integral to denitrification. In this regard, the integration of a TA system into a denitrification regulon may allow SUP05 to persist during periods of extreme NO_3^- limitation, analogous to other forms of nutritional stress response (e.g., amino acid starvation in *Escherichia coli*) (*30*).

As the number of studies surveying OMZ community structure increases, the ubiquity and abundance of SUP05 becomes apparent. Analysis of the SUP05 metagenome, together with water-column disposition of pelagic SUP05 with respect to H_2S and NO_3^- gradients, resolves a chemolithoautotrophic metabolism based on oxidation of reduced sulfur compounds with NO_3^- through multiple and highly regulated bioenergetic routes. Although pelagic distribution of SUP05 in Saanich Inlet and African shelf waters is predicated on the basis of vertical H_2S and NO_3^- gradients, the presence of this lineage in nonsulfidic OMZs (e.g., ENP and ESP) emphasizes the need to more fully resolve the chemical speciation of sulfur compounds with respect to SUP05 physiology and population structure. Moreover, the contribution of SUP05-mediated denitrification to the present unbalanced nitrogen cycle and the potential interplay with anaerobic ammonia-oxidizing bacteria within sulfidic and nonsulfidic OMZs remains to be investigated.

Paradoxically, as "dark" primary producers, blooming SUP05 populations have the potential to fix CO_2 while simultaneously producing N_2O.

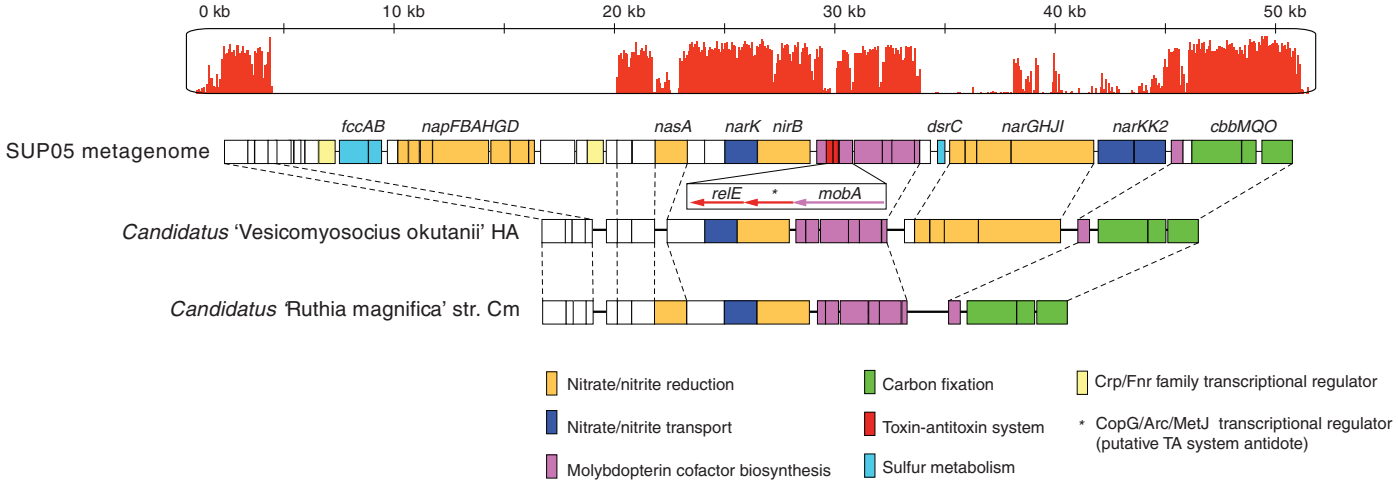

Fig. 4. Alignment of an ungapped region of a SUP05 metagenomic scaffold, encoding genes involved in nitrate and sulfur metabolism, with the corresponding genomic regions of symbiont reference genomes. The height of red bars corresponds to nucleotide similarity over conserved genomic regions. Proper scaffold assembly across this region was verified by full-length sequencing of two overlapping fosmids.

As habitat range increases with OMZ expansion and intensification, this role will only become more visible and significant. Therefore, the SUP05 metagenome provides a functional template for analysis of gene expression in relation to climatologically relevant biogeochemical transformations within oxygen-deficient oceanic waters. This information should prove useful in the development of monitoring tools to assess microbial community responses to OMZ expansion and intensification.

References and Notes

1. R. J. Diaz, R. Rosenberg, *Science* **321**, 926 (2008).
2. K. R. Arrigo, *Nature* **437**, 349 (2005).
3. A. Paulmier, D. Ruiz-Pino, *Prog. Oceanogr.* **80**, 113 (2008).
4. L. Stramma, G. C. Johnson, J. Sprintall, V. Mohrholz, *Science* **320**, 655 (2008).
5. F. A. Whitney, H. J. Freeland, M. Robert, *Prog. Oceanogr.* **75**, 179 (2007).
6. P. G. Brewer, E. T. Peltzer, *Science* **324**, 347 (2009).
7. B. M. Fuchs, D. Woebken, M. V. Zubkov, P. Burkill, R. Amann, *Aquat. Microb. Ecol.* **39**, 145 (2005).
8. D. Woebken, B. A. Fuchs, M. A. A. Kuypers, R. Amann, *Appl. Environ. Microbiol.* **73**, 4648 (2007).
9. H. Stevens, O. Ulloa, *Environ. Microbiol.* **10**, 1244 (2008).
10. G. Lavik *et al.*, *Nature* **457**, 581 (2009).
11. E. Zaikova *et al.*, *Environ. Microbiol.* 10.1111/j.1462-2920.2009.02058.x (2009).
12. N. Bano, J. T. Hollibaugh, *Appl. Environ. Microbiol.* **68**, 505 (2002).
13. M. Sunamura, Y. Higashi, C. Miyako, J. Ishibashi, A. Maruyama, *Appl. Environ. Microbiol.* **70**, 1190 (2004).
14. J. J. Anderson, A. H. Devol, *Estuar. Coast. Mar. Sci.* **1**, 1 (1973).
15. Materials and methods are available as supporting material on *Science* Online.
16. H. Kuwahara *et al.*, *Curr. Biol.* **17**, 881 (2007).
17. I. L. G. Newton *et al.*, *Science* **315**, 998 (2007).
18. G. Jost, M. V. Zubkov, E. Yakushev, M. Labrenz, K. Jurgens, *Limnol. Oceanogr.* **53**, 14 (2008).
19. C. G. Friedrich, F. Bardischewsky, D. Rother, A. Quentmeier, J. Fischer, *Curr. Opin. Microbiol.* **8**, 253 (2005).
20. J. Zopfi, T. G. Ferdelman, B. B. Jorgensen, A. Teske, B. Thamdrup, *Mar. Chem.* **74**, 29 (2001).
21. R. B. Cardoso *et al.*, *Biotechnol. Bioeng.* **95**, 1148 (2006).
22. C. Dahl *et al.*, *J. Bacteriol.* **187**, 1392 (2005).
23. R. D. Vetter, *Mar. Biol.* (Berlin) **88**, 33 (1985).
24. V. Stewart, Y. Lu, A. J. Darwin, *J. Bacteriol.* **184**, 1314 (2002).
25. H. Wang, C. P. Tseng, R. P. Gunsalus, *J. Bacteriol.* **181**, 5303 (1999).
26. S. Spiro, J. R. Guest, *FEMS Microbiol. Rev.* **6**, 399 (1990).
27. M. Mussmann *et al.*, *PLoS Biol.* **5**, e230 (2007).
28. D. P. Pandey, K. Gerdes, *Nucleic Acids Res.* **33**, 966 (2005).
29. D. J. Richardson, B. C. Berks, D. A. Russell, S. Spiro, C. J. Taylor, *Cell. Mol. Life Sci.* **58**, 165 (2001).
30. S. K. Christensen, M. Mikkelsen, K. Pedersen, K. Gerdes, *Proc. Natl. Acad. Sci. U.S.A.* **98**, 14328 (2001).

31. This work was performed under the auspices of the U.S. Department of Energy's Office of Science, Biological, and Environmental Research Program and by the University of California, Lawrence Berkeley National Laboratory, Lawrence Livermore National Laboratory under contract no. DE-AC02-05CH11231, Lawrence Livermore National Laboratory under contract no. DE-AC52-07NA27344, and Los Alamos National Laboratory under contract no. DE-AC02-06NA25396. This work was also supported by grants from the Natural Sciences and Engineering Research Council (NSERC) of Canada 328256-07 and STPSC 356988, Canada Foundation for Innovation (CFI) 17444; Canadian Institute for Advanced Research (CIFAR), and the Center for Bioinorganic Chemistry (CEBIC). D.A.W. was supported by NSERC, Killam Trust, and the Tula Foundation–funded Centre for Microbial Diversity and Evolution (CMDE). We thank M. Robert (Institute of Ocean Sciences, Sidney, BC, Canada), C. Payne, L. Pakhomova, and J. Granger (UBC) for help in sampling and chemical analyses and the captains and crews of the *CCGS John P. Tulley* and *HMS John Strickland* for logistical support. We thank the Joint Genome Institute, including K. Barry, S. Pitluck, and E. Kirton, for technical assistance and A. Page, K. Mitchell, and S. Lee in the Hallam laboratory for reading the manuscript. This metagenome project has been deposited at the DNA DataBank of Japan and European Molecular Biology Laboratory, and GenBank, under the project accession ACSG00000000. The version described in this paper is the first version, ACSG01000000. SSU rRNA gene sequences were deposited at GenBank under the accession numbers GQ345343-GQ351265, and fosmid sequences were deposited under the accession numbers GQ351266 to GQ351269 and GQ369726.

Supporting Online Material

www.sciencemag.org/cgi/content/full/326/5952/578/DC1
Materials and Methods
SOM Text
Figs. S1 to S7
Tables S1 to S4
References

22 April 2009; accepted 2 September 2009
10.1126/science.1175309

Pathogenesis of Chytridiomycosis, a Cause of Catastrophic Amphibian Declines

Jamie Voyles,[1]* Sam Young,[1] Lee Berger,[1] Craig Campbell,[2] Wyatt F. Voyles,[3] Anuwat Dinudom,[2] David Cook,[2] Rebecca Webb,[1] Ross A. Alford,[4] Lee F. Skerratt,[1] Rick Speare[1]

The pathogen *Batrachochytrium dendrobatidis* (*Bd*), which causes the skin disease chytridiomycosis, is one of the few highly virulent fungi in vertebrates and has been implicated in worldwide amphibian declines. However, the mechanism by which *Bd* causes death has not been determined. We show that *Bd* infection is associated with pathophysiological changes that lead to mortality in green tree frogs (*Litoria caerulea*). In diseased individuals, electrolyte transport across the epidermis was inhibited by >50%, plasma sodium and potassium concentrations were respectively reduced by ~20% and ~50%, and asystolic cardiac arrest resulted in death. Because the skin is critical in maintaining amphibian homeostasis, disruption to cutaneous function may be the mechanism by which *Bd* produces morbidity and mortality across a wide range of phylogenetically distant amphibian taxa.

Infectious disease can cause population declines (*1*), and potentially extinctions (*2*), if multiple variables create favorable conditions for severe outbreaks. A striking example is the global loss of amphibians due to chytridiomycosis (*1*, *3*, *4*). Despite an initial reluctance to accept disease as a direct cause of declines (*5*), *Batrachochytrium dendrobatidis* (*Bd*) is now recognized for its ability to spread rapidly though amphibian populations (*6*, *7*), infect numerous species (*1*, *6*), cause high rates of mortality (*6*, *8*), and persist even at low host densities (*7*, *9*). These disease characteristics render population recovery from chytridiomycosis especially difficult and provide strong evidence for disease-induced extinctions (*2*, *8*, *10*). However, the mechanism by which *Bd* kills amphibians is unknown.

The pathogenesis of chytridiomycosis has been difficult to determine because cutaneous fungal infections are rarely fatal without other predisposing factors (*11*). Furthermore, *Bd* is in a phylum of fungi not previously known as pathogens of vertebrates (*12*), it is confined to the superficial layers of the epidermis (*2*, *13*) with minimal host reaction to infection (*13*, *14*), and no consistent pathological changes in internal organs of diseased amphibians are detectable with light microscopy (*3*). Differential expression of peptidase genes suggests that *Bd* pathogenicity may have a genetic basis (*15*), but determining the proximate cause of death has been inherently challenging because multiple physiological systems shut down before death.

Amphibian skin is unique among terrestrial vertebrates because it is actively involved in the exchange of respiratory gases, water, and electrolytes (*16*–*19*). Because of the role of amphibian skin in maintaining osmotic balance, other studies have suggested that *Bd* might disrupt cutaneous osmoregulation (*3*, *20*). To test this hypothesis, we tracked the development of *Bd* infections in green tree frogs (*Litoria caerulea*), which are susceptible to chytridiomycosis in

[1]School of Public Health, Tropical Medicine and Rehabilitation Sciences, Amphibian Disease Ecology Group, James Cook University, Townsville, QLD 4811, Australia. [2]Discipline of Physiology, Bosch Institute, Faculty of Medicine, University of Sydney, Sydney, NSW 2006, Australia. [3]School of Medicine, Division of Cardiology, University of New Mexico, Albuquerque, NM 87131, USA. [4]School of Marine and Tropical Biology, Amphibian Disease Ecology Group, James Cook University, Townsville, QLD 4811, Australia.

*To whom correspondence should be addressed. E-mail: jamie.voyles@gmail.com

ERRATUM

Post date 30 April 2010

Reports: "Metagenome of a versatile chemolithoautotroph from expanding oceanic dead zones" by D. A. Walsh *et al*. (23 October 2009, p. 578). There are two changes to the names of sequences within tree 1 in Fig. 1A. The first two Eastern South Pacific clones are ESP60-K23I-54 (DQ810449), not ESP200-K23I-54, and ESP60-Khe2-29 (DQ810511), not K23II-30 (DQ810478).